Localized spin canting in partially inverted ZnFe$_2$O$_4$ fine powders

S. A. Oliver

Center for Electromagnetic Research, Northeastern University, Boston, Massachusetts 02115

H. H. Hamdeh and J. C. Ho

Department of Physics, Wichita State University, Wichita, Kansas 67260

Stoichiometric zinc ferrite fine powders showing long-range magnetic order to temperatures above 30 K have been prepared by the supercritical sol-gel method. The low-temperature magnetic behavior of the as-produced powder, and portions calcined at 500 and 800 °C, were determined by Mössbauer-effect measurements in an applied field of 7 T. The inversion parameter of the as-produced powder was 0.21, with those of the calcined powders being <0.05. A localized canted spin structure was found at 4.2 K, where spin canting was measured for both the Fe^{3+} moments aligned parallel and antiparallel to the applied field. The canting for antiparallel aligned spins vanished above the Néel temperature, where the fractional areas of the absorption peaks approached those expected from the inversion parameters. Spin canting persisted for the parallel moments to temperatures of 20–30 K, where the broadened sextets then showed collinear magnetic alignment. Slow relaxation processes were observed in Mössbauer spectra at 4.2 K, while the spectra was affected by the onset of fast relaxation processes at higher temperatures. The ability to adjust the inversion parameters in these powders make them excellent candidates for the study of long-range magnetic ordering in nearly antiferromagnetic spinel ferrites. [S0163-1829(99)10229-7]

INTRODUCTION

The spin structure in spinel ferrites is intricately connected to the cation occupancy of interstitial sites having either tetrahedral or octahedral symmetry within a close-packed oxygen lattice. Ferrimagnetic ordering occurs because the negative exchange interaction J_{AB} between magnetic cations occupying the tetrahedral (or A) sites and the octahedral (or B) sites dominates the negative intrasublattice exchange interactions J_{AA} and J_{BB}, causing each of the two magnetic sublattices on A sites and B sites to be aligned and frustrated. Early experiments on nonmagnetic cation substitution for iron in magnetite-based spinels showed that this two-sublattice model held only for cases where both the A-site and B-site magnetic sublattices were predominately occupied by magnetic cations.[1] A significant replacement of magnetic cations was seen to cause a reduction in sample magnetization, which was described as a spin canting mechanism by Yafet and Kittel.[2] Further dilution of magnetic ions provides a wonderful richness of magnetic behaviors, including antiferromagnetic, spin-glass, canted ferrimagnet, or more complex magnetic orderings, yielding results that have been used to construct magnetic phase diagrams as a function of magnetic cation occupancy of A and B sites.[3,4] In particular, noncollinear spin structures, such as a localized canted spin structure, can occur on either sublattice depending on the distribution of magnetic cations.

Diamagnetic zinc cations have often been used in substitutional studies of spinel spin structures, where a zinc cation replaces a magnetic cation on a tetrahedral site.[5] Stoichiometric zinc ferrite (ZnFe$_2$O$_4$) is a simple spinel where zinc cations occupy almost all of the tetrahedral sites due to their affinity for strong, nearly covalent, sp^3 bonding with oxygen anions. This leaves all the ferric iron ions on the octahedral

sites. Zinc ferrite is thus typically considered as a prototypic normal spinel, where normal refers to the case where the site occupancy of Zn^{2+} on B sites, or inversion parameter of the material, is zero. Magnetic ordering then arises from the weak J_{BB} exchange interaction, which yields a complex antiferromagnetic ordering near 10 K.[6] In practice, stoichiometric zinc ferrite in equilibrium approaches the prototypic normal spinel with only a very small inversion parameter.[7] Thus zinc ferrite provides an ideal system for the exploration of spin structures in a sparsely populated magnetic sublattice, except for the difficulty in obtaining significant inversion parameters in bulk materials. However, fine powders of zinc ferrite can show much larger inversion parameters than bulk zinc ferrite materials.[8] Such powders show a spontaneous magnetization to 30 K, with Mössbauer measurements showing a noncollinear spin structure to this temperature.[9]

Recently, fine powders of stoichiometric zinc ferrite produced by the supercritical sol-gel, or aerogel, processing method were shown to have magnetic properties at markedly higher temperatures than bulk zinc ferrite.[10] X-ray diffraction (XRD) measurements showed a substantial inversion parameter of 0.21.[11] Magnetization, Mössbauer-effect, and heat-capacity measurements all gave results indicative of long-range magnetic ordering to 30 K. The inversion parameters of portions of this starting powder were then modified through one of two methods. A greatly increased inversion parameter near 0.55 was obtained by ball-milling the starting powder, which resulted in a sample having a spontaneous magnetization at room temperature.[10] Meanwhile, calcining the powders at 500 and 800 °C reduced the inversion parameter below the resolution of Rietveld refinement methods, and improved the crystal structure. These powders were expected to have antiferromagnetic behavior, but instead showed substantial magnetization at elevated temperatures.

PRB <u>60</u>   3400

One question regarding these nonequilibrium zinc ferrite powders is the nature of the spin structure, or magnetic ground state. Given the sparse population of iron atoms in A sites in the near-normal calcined samples, the magnetic phase diagrams for spinels predict a spin-glass behavior.[3,4] However, neither the magnetization nor Mössbauer results showed indications for a spin-glass transition, although heat-capacity data were compatible with that of a spin glass.[12] Instead, the magnetic properties were masked by fast relaxation processes, such as superparamagnetism, where the Mössbauer spectra collapsed to an electric quadrupole doublet at temperatures where a substantial magnetization was still observed by magnetometry measurements. Even at temperatures of 25 K the existence of fast relaxation processes arising either from superparamagnetic effects or collective magnetic excitations processes was noted in the Mössbauer spectra through the presence of both line broadening and an interior doublet. These processes were presumed to arise from thermal activation of small, weakly coupled clusters of magnetic moments.[13–15]

In order to explore the nature of the magnetic spin structures in these partially inverted zinc ferrite powders, this work reports on results from Mössbauer-effect measurements that were taken in a 7-T magnetic field. This field is sufficiently strong to suppress fast relaxation processes in these powders at low temperatures, allowing determination of the underlying spin structures. Here, we show that local spin canting is clearly apparent at 4.2 K for Fe^{3+} cations occupying the octahedral sites, for both spins aligned parallel and antiparallel to the applied field. Above the Néel temperature the absorption from the antiparallel octahedral site moments collapses, leaving only antiparallel absorbers corresponding to Fe^{3+} cations occupying tetrahedral sites. One unexpected result is the retention of local spin canting for the structurally refined powders that have very low inversion parameters, which might be expected to have antiferromagnetic behavior.

EXPERIMENTAL

Fine zinc ferrite powders were produced by the critical sol-gel processing, or aerogel, method.[11] Zinc acetate and ferric acetylacetonate precursors were mixed at a Zn:Fe ion ratio of 1:2, and then dissolved in methanol hydrolyzed with 1.2 times the stoichiometric amount of water. This mixture was then transferred to a glass vessel and placed in an autoclave. Additional methanol was added such that the mixture attained the critical point of methanol (512.6 K, 82.5 bars) upon heating the closed system to a temperature of 524 K at a rate of 15 K/min. Then the pressure was slowly relieved at constant temperature, with the autoclave finally being cooled while venting with flowing nitrogen gas to remove any remaining methanol vapor. The fine aerogel powder was then removed from the chamber. Portions of this powder were calcined at 500 and 800 °C for 2 h, yielding the materials examined in this work.

The sample crystallographic properties were determined by powder x-ray-diffraction (XRD) measurements,[11] with the spinel structure being confirmed by extended x-ray-absorption fine-structure (EXAFS) measurements. All samples were found to be single phase $ZnFe_2O_4$, with the exception of the as-produced powder that had an amorphous
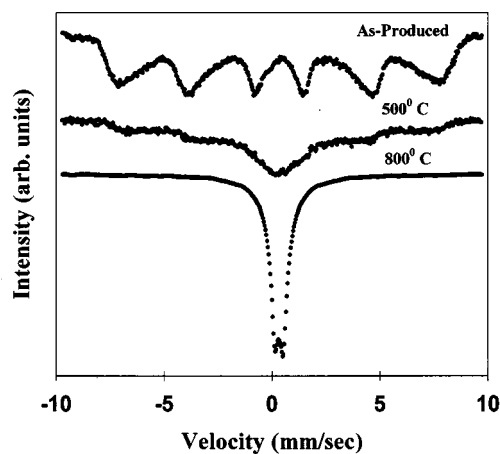

FIG. 1. Mössbauer-effect data at 25 K with no applied field for all samples.

component. The as-produced powder had a lattice constant of 0.844 11 nm, approximately 0.1% larger than that of the reference pattern. A distinct sharpening of the diffraction pattern lines occurred for calcined samples, as expected with onset of grain growth, improvements in crystallographic ordering, and the reduction in microstrains. Rietveld refinement provided an inversion parameter of 0.21 for the as-produced powder sample, and indicated near-zero inversion parameter values for the calcined samples.

Powder particle sizes were determined from the x-ray-diffraction patterns using Scherrer's method, and yielded values of 8.1, 13.9, and 39 nm for the as-produced sample, and samples calcined at 500 and 800 °C, respectively.[11] The particle size distribution was measured from bright field micrographs for the as-produced powder, and yielded an average diameter of 14 ± 4 nm. This result implies that the crystallites deduced from Scherrer's method may reside in an amorphous matrix, at least for the as-produced sample.

Mössbauer-effect measurements were taken in transmission mode, with the ^{57}Co source mounted in a standard constant acceleration drive unit. Powder samples were prepared between layers of tape, and were mounted on the finger of a liquid ^4He flow cryostat which provided for temperature control from 4.2 K to room temperature. The sample temperature was monitored using a Cernox thermoresistor mounted on the sample block. The sample assembly was then placed in the bore of a 7-T superconducting solenoid magnet, such that the direction of gamma ray propagation coincided with the magnetic-field axis. All measurements were calibrated with respect to α-Fe.

RESULTS AND DISCUSSION

The presence of magnetic behavior for all three samples at temperatures above the 10-K Néel temperature of equilibrium zinc ferrite is demonstrated by the Mössbauer spectra taken at 25 K shown in Fig. 1. Here the spectra for both the as-produced sample and the sample calcined at 500 °C show the sextet typical for the hyperfine splitting of iron, although the absorption lines for both spectra show considerable broadening. Even the sample calcined at 800 °C shows broadened shoulders of the electric quadrupole doublet, meaning the hyperfine magnetic splitting has not yet fully
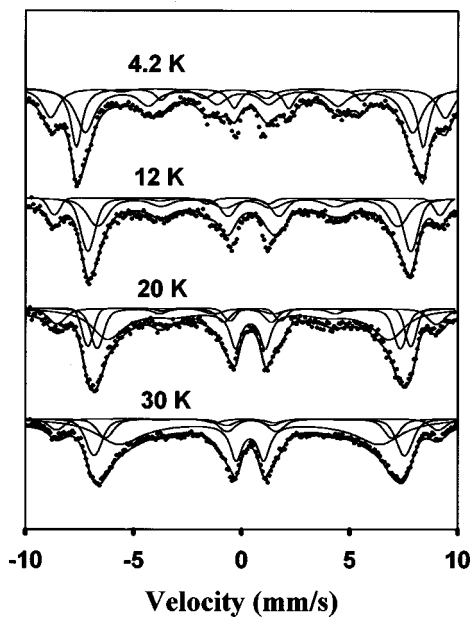
FIG. 2. Mössbauer-effect data on the as-produced sample in a 7-T applied field at the temperatures listed. Solid lines are fits to the spectra.

FIG. 3. Mössbauer-effect data on the sample calcined at 500 °C in a 7-T applied field at the temperatures listed. Solid lines are fits to the spectra.

collapsed. However, as noted above, interpretation of the Mössbauer data is hindered by absorption line broadening caused by thermal effects, such as superparamagnetism and collective magnetic excitations. With increasing measurement temperature, the onset of superparamagnetic effects will act to collapse the sextet structure since the fixed Mössbauer interaction time becomes greater than the relaxation times of the local magnetization. Meanwhile, collective magnetic excitations arising from moment fluctuations about the local easy axis will not collapse the sextet, but will act instead to reduce the measured hyperfine magnetic field (HMF). Here again, the severity of this effect depends upon the local fluctuation relaxation time relative to the Mössbauer interaction time.

Thermal fluctuation effects can be suppressed by the application of a strong magnetic field, especially for low-temperature measurements. Thus Mössbauer measurements were taken on all three samples as a function of temperature while at a fixed 7-T magnetic field. Results from such measurements are shown in Figs. 2–4, which show Mössbauer effect spectra for the as-produced sample, and samples calcined at 500 and 800 °C, respectively. These figures also show the fitting results, which will be explained later. All of the spectra now show distinct hyperfine sextets. The significance of thermal fluctuations for these samples is demonstrated by comparing the 25-K spectra of the sample calcined at 500 °C in Fig. 3 with the corresponding spectra in Fig. 1, where distinct hyperfine splitting is now observed upon application of the magnetic field.

Qualitatively, spectra taken on the three samples at the same temperature are similar, with the major distinctions being the higher intensities of the $\Delta m = 0$ (second and fifth) lines for the two calcined samples relative to the as-produced sample, while the as-produced sample shows a much more distinct splitting of the outermost (first and sixth) lines relative to the calcined samples. All of the spectra taken at 4.2 K
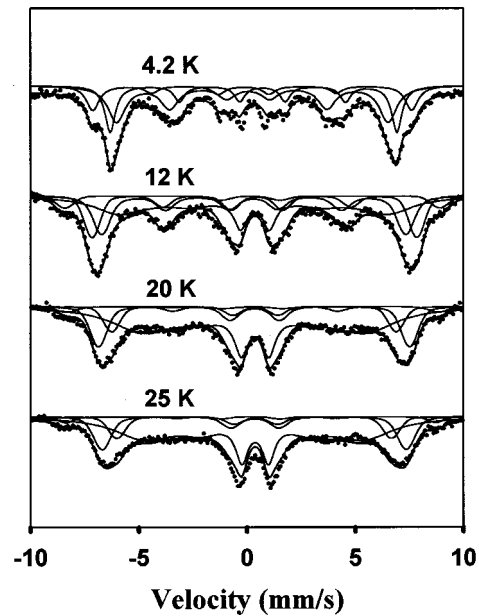
have split outermost peaks, as expected from Zeeman splitting of the majority and minority spin sublattices, where the majority spin sublattice is aligned parallel to the applied magnetic field (H), while the minority spin sublattice lies antiparallel to H. Slight asymmetries are also apparent for the outermost lines, indicative of chemical ordering. The resolution of these asymmetries further indicate that thermal broadening has been suppressed. The changes between spectra taken on the same sample at increasing temperatures follows the same trend for each powder, as the widths of the outermost absorption lines are seen to increase, while the innermost lines become sharper and more distinct. Moreover,
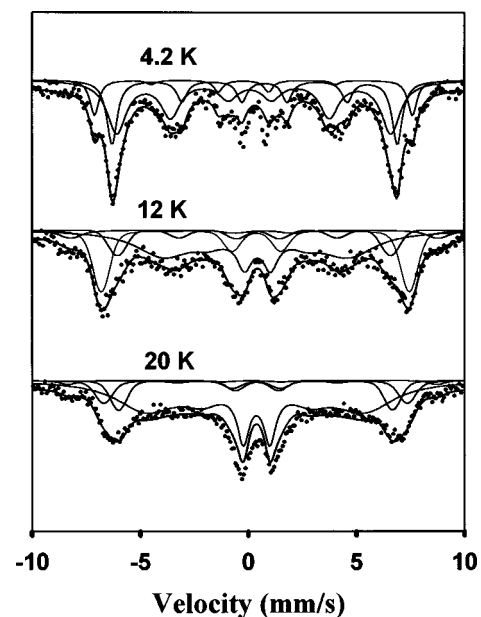

FIG. 4. Mössbauer-effect data on the sample calcined at 800 °C in a 7-T applied field at the temperatures listed. Solid lines are fits to the spectra.

TABLE I. Sextet fitting results for 4.2-K Mössbauer spectra.

Powder	Sextet	HMF (kG)	IS (mm/s)	A_s ±0.01	z
As-produced	A	557	0.28±0.04	0.24	0.11±0.05
	$B1$	487±1	0.35±0.03	0.76	0.20±0.03
	$B2$	463±2	0.32±0.06		0.37±0.04
Calcined @ 500 °C	A	547±2	0.30±0.06	0.20	0.28±0.07
	$B1$	494±1	0.36±0.04	0.80	0.34±0.04
	$B2$	470±2	0.32±0.06		0.61±0.06
Calcined @ 800 °C	A	542±2	0.30±0.06	0.16	0.12±0.10
	$B1$	493±2	0.35±0.06	0.84	0.33±0.07
	$B2$	472±2	0.32±0.06		0.68±0.10

the second and fifth lines almost disappear with rising measurement temperatures. Most important, the existence of the second and fifth lines in the presence of the 7-T applied field is a definitive indicator for spin canting in these powders.

A quantitative analysis of the sample magnetic properties was done by least-squares fitting the Mössbauer spectra to a summation of three or four hyperfine sextets. The sextet corresponding to the peaks that are split to higher velocities upon application of the external magnetic field are denoted as A, following the nomenclature used previously for the minority spin sublattice in spinels.[5] Thus all of the absorbers contributing to A consist of ^{57}Fe ions that have spin components antiparallel to the applied field. Depending on the temperature, the contributors to this spectra can include both ^{57}Fe ions occupying tetrahedral lattice sites and ions on the octahedral sites having reversed moments. Indeed, the possibility for contributions from absorbers occupying either site makes the evolution of the A-sextet spectra a good indicator for the behavior of the magnetic system.

While the peaks split to higher velocities with H were assigned to sextet A, those peaks split to lower velocities with H are denoted spectra B. Here, all contributors to the absorption in the B sextets are presumed to be ^{57}Fe ions occupying octahedral sites as part of the majority spin sublattice. In practice, it was found that these peaks were best fit by a pair of sextets having different hyperfine magnetic-field values and isomer shifts (IS), analogous to the fitting procedures used previously by researchers who divided the sextet into contributions from ^{57}Fe cations having different local environments.[5,16] These sextets are labeled $B1$ and $B2$, where the label $B2$ was assigned to the broader absorption peak having lower HMF values. Both of these sextets incorporate cations having a broad range of local magnetic environments.[5,16]

The least-squares-fitting procedure was done using user defined functions within the Jandel PeakFit program. The free parameters for each sextet in the fit consisted of the position, height and width of the first peak, the HMF, the quadrupole electric field, and the ratio of the relative areas under the second and fifth ($A_{2,5}$) and first and sixth ($A_{1,6}$) peaks $z=A_{2,5}/A_{1,6}$. One fitting constraint held the area under each pair of Lorentzian peaks ($A_{1,6}$, $A_{3,4}$) in a sextet in the theoretical ratio $1:\frac{1}{3}$. The fitting parameters were allowed to vary within the constraint above to obtain the best least-squares fit of the data. Fit results for each of the three sextets

are plotted as solid lines for each spectra in Fig. 2–4, along with their sum.

Thermally induced relaxation processes were sufficiently suppressed at 4.2 K and 7 T to allow good fits to Lorentzian absorptions to be made to the outermost peaks of each sextet. However, the inner lines were not fitted as accurately due to their shifting to lower velocities. This shift in the innermost peaks was suggestive of the presence of an additional absorption mechanism in the spectra, such as a slow magnetic relaxation process between magnetic-field-split electronic states that have differing occupation levels.[17]

Parameters extracted from fits to the 4.2-K data are tabulated in Table I, which lists results for the HMF, IS, relative areal fraction (A_s) for the A and B ($B=B1+B2$) sextets, and the parameter z. The measured isomer shift values on the A site are comparable to those previously determined for Fe^{3+} on tetrahedral sites,[18,19] while the values listed in Table I for Fe^{3+} occupying B sites also compare well with the value of 0.35 mm/sec found previously.[5,19] When combined, the isomer shift values of Table I indicate that good charge compensation, and hence stoichiometry, is maintained in the powders, since isomer shift values near 0.65 mm/sec are commonly measured when the octahedral sites are occupied both by ferric and ferrous iron cations, as in the case of mixed-valence magnetite (Fe_3O_4). Similarly, the HMF values agree well with results found by Dickof, Schurer, and Morris for high-field Mössbauer-effect measurements on $Zn_xFe_{3-x}O_4$ powders where $x=0.8$.[5] In particular, they obtained a HMF value of 566 kOe for ^{57}Fe moments that were aligned opposite to the 50-kOe applied field, and HMF values near 470 kOe for moments aligned with H.[5] In addition, Ligenza et al. obtained a HMF value of 559 kOe from high-field (60 kOe) measurements of ^{57}Fe ions occupying A sites in partially inverted polycrystalline $ZnFe_2O_4$ samples, while neighbors of these sites had lower HMF values.[16]

A direct measure of the spin canting in these powders is given by the nonzero $A_{2,5}$ peak intensities apparent in Figs. 2–4, and as listed as z in Table I for samples measured at 4.2 K. Here, z provides the degree of collinearity of the magnetic moments in that sextet relative to the applied magnetic field. For reference, $z=0$ when all spins are parallel or antiparallel to H, and will be nonzero if any spins have a component transverse to H up to the maximum value of $z=\frac{4}{3}$ obtained for the pure transversely oriented case. Measurements on

ideal normal ferrimagnetic materials will not have either the second or fifth peaks present, and thus have $z=0$. As seen from Table I, these powders show large values of z for all three of the fitted sextets, where the broader fit sextet $B2$ shows a much larger z parameter than either the A or $B1$ sextets. This particular relationship between the z parameters of the three sextets was found to hold for data fits at all temperatures.

Least-squares fitting of the data taken at higher temperatures was complicated by the broadening and collapsing of the peaks in the spectra. Thus it was necessary to add an additional spectra to fit the data taken on the as-produced powder at 20 K and above, and for data collected for both calcined powders at 12 K and above. The same fit parameters were used for this additional sextet as for the A and B sextets, except that the relaxation time was chosen to be comparable to the Mössbauer interaction time such that the sextet had the shape of a collapsing spectra.[17] This sextet physically represents the significant fraction of ^{57}Fe ions in the powder that are affected by thermally induced fluctuations, and indicates that the 7-T external field can no longer suppress these relaxation effects at these slightly higher temperatures. The effect of these fluctuations is to shift considerable intensity from the outermost peaks to the inner peaks, and in particular to the region about the second and fifth peaks, as can be seen in the high-temperature spectra in Figs. 2–4. This will lead to an increase in the standard error deduced from the fitting procedure for z. However, the spectral weight of this collapsed spectra does not obscure the resolution of the outermost peaks into A and B sextets, although they also have larger standard errors compared to the 4.2-K measurements. For simplicity of analysis, the area under this collapsed fit spectrum was added to the B sextet while determining A_s, such that the A-sextet fractional area will be slightly undercounted.

Estimates for the mean spin canting angle for moments in the A sextet and B sextets can be obtained from the relationship

$$\Phi = \arcsin \left[\frac{\frac{3}{2}z}{1+\frac{3}{4}z} \right]^{1/2}, \quad (1)$$

where $\Phi=0$ corresponds to the spins being parallel with H. From Table I, the deduced spin canting angles for the A sextets of all three powders lie in the range from 140°–160°, where these canting angles are assumed to be nearly antiparallel to H because the HMF split to higher fields with H for this sextet. The mean canting angle for the $B1$ sextet lies between 30° and 40° for all three samples, with that of $B2$ always showing a higher canting angle ranging from 40°–55°. With increasing temperature the area of $A_{2,5}$ for the A sextet drops to zero at 12 K and thus the spin canting angle converges to 180°, indicating the collapse of canting for the antiparallel spins. In contrast, the $A_{2,5}$ peaks for the B sextets do not disappear at 12 K, but instead slowly decrease with temperature so that the mean spin canting angle for the B sextet slowly approaches alignment with H.

This pattern of rapid change in the $A_{2,5}$ peak height with increasing temperature is indicative for the existence of a localized canted spin system.[3,5] The source of this behavior has been attributed to the onset of rapid fluctuations of transverse component of the canted magnetic moments while the component longitudinal along the applied magnetic field remains frozen.[3] At the lowest temperatures the relaxation time of fluctuations for the transverse spin component is slow compared to the Mössbauer measurement time, permitting measurement of this spin component. Upon heating the transverse component of the local spin moment thaws, such that the transverse spin relaxation time becomes faster than the Mössbauer measurement time, effectively time averaging this component to zero.

One notable feature of these zinc ferrite powders is the observation of spin canting on both the A and B sextets. This result is in contrast to those from $ZnFe_2O_4$ and other Fe^{3+} spinel systems studied previously where spin canting was measured only on the B sites.[3,16] However, most of the Fe^{3+} spinel systems had large inversion parameters, such that the development of the localized spin canting behavior could be considered to be a perturbation of the spinel ferrimagnetic ordering. In contrast, the development of spin canting behavior for the low inversion parameter calcined powders, in particular, could be considered to be a perturbation of spinel antiferromagnetic ordering. A large majority of the Fe^{3+} ions then occupy octahedral sites and do not have magnetic cations on neighboring tetrahedral sites. These moments will order antiferromagnetically with respect to the net moment of the neighboring cations. In turn, the orientation of these neighboring moments will depend upon the orientation of other spins in their local environments, which may be canted or reversed because of the effects of neighboring Fe^{3+} ions on tetrahedral sites, defects, or their presence on the particle surface. Indeed, it has been previously estimated that for inversion parameters below $x=0.05$ the orientation of each weakly exchange-coupled B-site spin is dependent on the orientation of neighbor spins out to at least 10 to 20 nearest neighbors because of multiple spin reversals.[5] In this scenario, the distribution of spins at the particle surface may greatly affect the magnetic structure of a considerable volume fraction of the particle, introducing a particle size effect. Thus the orientation of a weakly coupled B site will be canted with respect to the applied field, and thus contribute to the absorption of the $A_{2,5}$ peaks of either the A and B sextets. In contrast, the few Fe^{3+} ions on tetrahedral sites will be antiferromagnetically exchange coupled to a full shell of neighboring Fe^{3+} ions on B sites through the stronger J_{AB} interaction, and will thus have small or zero canting angles. Thus the observed spin canting in the A sextet can be fully attributed to the reversed B-site moments. It is then not unexpected that the spin canting observed for the A sextet vanishes above the Néel temperature.

The major contribution to the outer peaks of the A and B sextets above 10 K will arise from ^{57}Fe ions coupled by the J_{AB} exchange interaction. This is demonstrated by the temperature dependence of the relative areal fractions (A_S) of the A and B sextets. For high-field Mössbauer-effect measurements on ferrimagnetic spinel ferrites, the value of (A_S) for the A sextet equals half the inversion parameter. Hence, inversion parameter values of $x=0.48$, 0.40 and 0.32 could be obtained from Table I, which greatly exceeds the results extracted from structural measurements since the A sextet contains a significant contribution from reversed B-site mo-

ments below 10 K. However, values for the areal fraction extracted from fits to higher temperature measurements show a sharp reduction in the A-sextet areal fraction. This process is not measured as a discrete transition, nor does it show a distinct Néel temperature, because of the distribution of local magnetic environments around the cations. Indeed, such a transition has been directly measured by the calorimetric measurements of Ref. 12, which shows the magnetic heat capacity to have broad peaks centered at temperatures below 10 K for all three samples. As may be expected, the powder calcined at 800 °C showed the narrowest, most defined peak in magnetic heat capacity, although the tails of the magnetic heat capacity data extended to 30 K for all three samples.[12]

The A-sextet A_S value has previously been found to be a good measure of the inversion parameter upon the disappearance of spin canting on the B sites.[3] Using this method inversion parameters can be deduced from the high-temperature Mössbauer fit results, yielding $x=0.14$, 0.05, and 0.03 for the as-produced, 500 and 800 °C samples, respectively. However, these values underestimate the inversion parameter since the fits of the Mössbauer spectra at higher temperatures are affected by the fast relaxation processes, although they are in reasonable agreement with values found from the x-ray-diffraction measurements. It should be noted that the Mössbauer deduced inversion parameter for the as-produced sample matches the XRD value of $x=0.21$ for 12-K measurements, where fast relaxation processes are not significant while the A-sextet canting has vanished.

CONCLUSION

Low-temperature Mössbauer-effect measurements taken at high magnetic fields have identified the magnetic spin structure of a series of fine zinc ferrite powders as corresponding with a localized canted spin structure. Second and fifth peaks were distinctly observed for the Mössbauer ab-

sorption sextets split both to higher and lower velocities upon application of the applied field, directly indicating the presence of canted spins in those sextets. These canted spins were identified as arising from Fe^{3+} moments on the octahedral sites (B sites) that were aligned either parallel or reversed to the applied field. The reversed B-site contribution vanished near the Néel temperature. The parallel B-site canted spin structure collapsed at temperatures near 20, 25, and 30 K for the samples calcined at 800 and 500 °C, and the as-produced powder sample respectively. The inversion parameters found from the areal fractions of the Zeeman split sextets upon collapse of the reversed B-site canting approximated those found from x-ray-diffraction results. Well defined sextets showing collinear magnetic ordering were present at the higher temperatures, although the outermost peaks were broadened by fast relaxation processes. Given the small inversion parameters and particle sizes of the calcined powders the spin structure at the particle surface may be important in determining the particle magnetic structure.

The zinc ferrite aerogel fine powders measured here appear to be excellent candidates for future experimentation on both the properties of spin structures in low inversion parameter materials, and also the effects of surface spin structures on net particle properties. In contrast to most divalent-cation substitutional studies, these materials are being perturbed from an antiferromagnetic spin state. In addition, the ability to readily adjust the inversion parameter and particle size of a simple spinel powder containing only ferric iron and diamagnetic zinc cations will greatly simplify analyses of the complex spin structures observed in spinel ferrites.

[1] C. Guillaud and M. Roux, C.R. Acad Sci. Paris **228**, 1110 (1949).

[2] Y. Yafet and C. Kittel, Phys. Rev. **87**, 290 (1952).

[3] J. M. Dormann and M. Nogues, J. Phys.: Condens. Matter **2**, 1223 (1990).

[4] J. M. D. Coey, Can. J. Phys. **65**, 1210 (1987).

[5] P. A. Dickof, P. J. Schurer, and A. H. Morrish, Phys. Rev. B **22**, 115 (1980).

[6] U. König, E. F. Bertaut, Y. Gros, M. Mitrikov, and G. Chol, Solid State Commun. **8**, 759 (1970).

[7] W. Schiessl, W. Potzel, H. Karzel, M. Steiner, G. M. Kalvius, A. Martin, M. K. Krause, I. Halevy, J. Gal, W. Schäfer, G. Will, M. Hillberg, and R. Wäppling, Phys. Rev. B **53**, 9143 (1996).

[8] T. Kamiyama, K. Haneda, T. Sato, S. Ikeda, and H. Asano, Solid State Commun. **81**, 563 (1992).

[9] T. Sato, K. Haneda, M. Seki, and T. Iijima, Appl. Phys. A: Solids Surf. **50**, 13 (1990).

[10] H. H. Hamdeh, J. C. Ho, S. A. Oliver, R. J. Willey, J. Kramer, Y. Y. Chen, S. H. Lin, Y. D. Yao, M. Daturi, and G. Busca, IEEE Trans. Magn. **31**, 3808 (1995).

[11] H. H. Hamdeh, J. C. Ho, S. A. Oliver, R. J. Willey, G. Oliveri, and G. Busca, J. Appl. Phys. **81**, 1851 (1997).

[12] J. C. Ho, H. H. Hamdeh, Y. Y. Chen, S. H. Lin, Y. D. Yao, R. J. Willey, and S. A. Oliver, Phys. Rev. B **52**, 10 122 (1995).

[13] Y. Ishikawa, J. Phys. Soc. Jpn. **17**, 1877 (1962).

[14] V. G. Harris, N. C. Koon, C. M. Williams, Q. Zhang, M. Abe, and J. P. Kirkland, Appl. Phys. Lett. **68**, 2082 (1996).

[15] S. A. Oliver, V. G. Harris, H. H. Hamdeh, and J. C. Ho (unpublished).

[16] S. Ligenza, M. Lukasiak, Z. Kucharski, and J. Suwalski, Phys. Status Solidi B **117**, 465 (1983).

[17] H. H. Wickman, in *Mössbauer Effect Methodology*, edited by I. J. Graverman (Plenum Press, New York, 1996), Vol. II, p. 39.

[18] T. Kanzaki, K. Kitayama, and K. Shimokoshi, J. Am. Chem. Soc. **76**, 1491 (1993).

[19] C. P. Marshall and W. A. Dodge, Am. Mineral. **69**, 928 (1984).